Biosensors and Bioelectronics 34 (2012) 125–131

Contents lists available at SciVerse ScienceDirect

Biosensors and Bioelectronics

journal homepage: www.elsevier.com/locate/bios

Electrochemical sensor based on nitrogen doped graphene: Simultaneous determination of ascorbic acid, dopamine and uric acid

Zhen-Huan Sheng[a,b], Xiao-Qing Zheng[a], Jian-Yun Xu[a], Wen-Jing Bao[a], Feng-Bin Wang[a], Xing-Hua Xia[a,*]

[a] State Key Laboratory of Analytical Chemistry for Life Science, School of Chemistry and Chemical Engineering, Nanjing University, Nanjing 210093, China
[b] School of Chemistry and Chemical Engineering, Huaiyin Normal University, Huai'an 223300, China

ARTICLE INFO

Article history:
Received 14 November 2011
Received in revised form 21 January 2012
Accepted 24 January 2012
Available online 2 February 2012

Keywords:
Nitrogen doped graphene
Electrochemical sensor
Simultaneous determination
Ascorbic acid
Dopamine
Uric acid

ABSTRACT

Nitrogen doped graphene (NG) was prepared by thermally annealing graphite oxide and melamine mixture. After characterization by atomic force microscopy and X-ray photoelectron spectroscopy etc., the electrochemical sensor based on NG was constructed to simultaneously determine small biomolecules such as ascorbic acid (AA), dopamine (DA) and uric acid (UA). Due to its unique structure and properties originating from nitrogen doping, NG shows highly electrocatalytic activity towards the oxidation of AA, DA and UA. The electrochemical sensor shows a wide linear response for AA, DA and UA in the concentration range of 5.0×10^{-6} to 1.3×10^{-3} M, 5.0×10^{-7} to 1.7×10^{-4} M and 1.0×10^{-7} to 2.0×10^{-5} M with detection limit of 2.2×10^{-6} M, 2.5×10^{-7} M and 4.5×10^{-8} M at $S/N = 3$, respectively. These results demonstrate that NG is a promising candidate of advanced electrode material in electrochemical sensing and other electrocatalytic applications.

1. Introduction

Carbon-based materials, especially carbon nanotubes (CNTs) and graphene discovered during the past two decades have been shown to be the hot topics of materials research. CNTs as nanoscaled building blocks have been employed for sensors, electronic devices (Banks et al., 2006; Deng et al., 2009a) etc. Currently, graphene emerging as a "superstar" material has also attracted tremendous attentions due to its unique structure and electronic properties (Allen et al., 2010; Rao et al., 2009). Researches on graphene in field of nanoelectronics (Pang et al., 2009; Wang et al., 2010a), biosensors (Shang et al., 2008; Tang et al., 2009; Shao et al., 2010; Guo et al., 2010a), and energy storage (Zhou et al., 2010; Elias et al., 2009) have been greatly developed. Due to the demands of investigation in these areas, different approaches have been developed to synthesize graphene with various microstructures. For example, chemical vapor deposition (CVD) was commonly used to prepare graphene (Kim et al., 2009; Reina et al., 2009). In this approach, the metal catalysts are usually incapsulated in the products, which makes the explanation of their intrinsic electrocatalytic properties difficult as in the case of CNTs (Jones et al., 2007; Pumera, 2007).

Chemical doping with heteroatoms such as nitrogen or boron atoms is an effective strategy to modulate electronic properties and surface chemistry for carbon materials (Zhou et al., 2000). For instance, nitrogen atoms can be easily doped into carbon structures via forming C—N bonds due to the similarity of atomic size and five-valence-electron structure. To date, nitrogen doped CNTs (N-CNTs) have been successfully prepared by CVD in the presence of nitrogen containing species (i.e., NH_3 and pyridine), and by pyrolysis of metal complexes with macrocycles containing nitrogen atoms (Lee et al., 2009; Gong et al., 2009). The resultant N-CNTs show much higher sensitivity in biosensing applications and excellent electrocatalytic activity towards oxygen reduction reaction (ORR) (Deng et al., 2009b; Xu et al., 2010). Owing to the structural similarity of CNTs and graphene, the doping methods for CNTs have been directly extended to prepare nitrogen doped graphene (NG) (Panchakarla et al., 2009; Wang et al., 2009a; Guo et al., 2010b). Wang et al. (2009a) reported NG with *n*-type semiconductive properties could be obtained through electrothermal reactions in ammonia gas. Qu et al. (2010) first reported that NG possesses much better electrocatalytic activity towards ORR, long time stability, and tolerance to crossover effect than platinum in alkaline fuel cells. Recently, it has been also reported that NG can promote the electrochemical reduction of hydrogen peroxide (H_2O_2) and direct electron transfer kinetics of glucose oxidase (Wang et al., 2010b). As a result, detection of glucose can be achieved by determining H_2O_2 generated from the enzymatic reaction in the presence of O_2. We recently

* Corresponding author. Tel.: +86 25 83597436; fax: +86 25 83597436.
E-mail address: xhxia@nju.edu.cn (X.-H. Xia).

0956-5663/$ – see front matter © 2012 Elsevier B.V. All rights reserved.
doi:10.1016/j.bios.2012.01.030

reported a facile approach to synthesize NG by thermally annealing a mixture of graphite oxide and melamine (Sheng et al., 2011) and the NG also show highly catalytic activity towards ORR in alkaline solution.

Ascorbic acid (AA), uric acid (UA) and dopamine (DA) play important roles in physiological function of organisms. The deficiency or maladjustment of their levels may lead to the symptoms of many diseases such as cancer, Parkinson's disease and cardiovascular disease (Arrigoni and De Tullio, 2002; Heien et al., 2005; Dutt and Mottola, 1974). Hence, determination of AA, DA and UA is of great importance for developing nerve physiology, making diagnosis and controlling medicine. However, in real systems, AA, DA and UA usually coexist in the extra cellular fluid of the central nervous system and serum. Electrochemically individual and/or simultaneous determinations of them on traditional electrodes are very difficult since they usually foul the detection electrodes and their oxidation potentials are severely overlapped. To these problems to be addressed, various approaches have been proposed to individually determine these biomolecules (Chen et al., 2009; Liu et al., 2008a; Han et al., 2010). Recent reports demonstrated that graphene based electrodes could be used to selectively determine DA in the existence of AA (Guo et al., 2009; Wang et al., 2009b). In this work, on the basis of synthesis, NG's electrocatalytic activity towards AA, DA and UA will be systematically studied. It is found that the high electrocatalytic activity of NG towards these three molecules originates from its unique geometric structure and properties. The NG-based electrochemical sensor can be used to simultaneously determine AA, DA and UA with high selectivity and sensitivity.

2. Experimental

2.1. Reagents and materials

Graphite powder (99.9995% purity, −100 mesh, briquetting grade, mesh) was purchased from Alfa Aesar. Melamine was bought from Sinopharm Chemical Reagent CO. Ltd (China), and recrystallized with water prior to use. Ascorbic acid was bought from Sinopharm Chemical Reagent CO., Ltd (China), dopamine and uric acid were bought from Sigma and used as received. Analytical grade H_2SO_4, $KMnO_4$, N,N-dimethyl formamide (DMF) were purchased from Nanjing Chemical Reagent CO. Ltd (China). All solutions were prepared with Millipore water having a resistivity of 18.2 MΩ (Purelab Classic Corp., USA). AA, DA and UA solutions were freshly prepared in phosphate buffer solutions (PBS) prior to use.

2.2. Instruments and measurements

Atomic force microscopy (AFM) images of NG were collected on an Agilent 5500 AFM/SPM system. Imaging was performed in tapping mode under ambient conditions. The morphology of NG was also characterized on a field-emission scanning electron microscope (FE-SEM, S-4800, Hitachi, Japan) at an accelerating voltage of 10 kV and a transmission electron microscopy (TEM, JEM-2100, JEOL, Japan) with a 200 kV accelerating voltage. Room-temperature Raman spectrum was recorded using a micro-Raman system (Renishaw InVia, UK) with an excitation wavelength of 514 nm. X-ray photoelectron spectroscopy (XPS) analyses were carried out on a Thermo Fisher X-ray photoelectron spectrometer system equipped with Al radiation as a probe (K-alpha, Thermo Fisher Scientific, USA) at a chamber pressure of 5×10^{-9} Torr. The source power was set at 72 W, and pass energies of 200 eV for survey scans and 50 eV for high-resolution scans were used. Electrochemical measurements were performed on a CHI 900 electrochemical workstation (CH Instruments, USA). A conventional three-electrode system was used throughout the measurements. The working electrode was a bare or modified glassy carbon electrode (GCE, ϕ = 3.0 mm), a platinum wire as the counter electrode and an Ag/AgCl electrode as the reference. Individual or simultaneous determination of AA, DA and UA was carried out using differential pulse voltammetry (DPV).

2.3. Synthesis of nitrogen doped graphene

In a typical procedure, the mixture of graphite oxide (Guo et al., 2009) and melamine with a mass ratio of 1:10 was placed in the center of a corundum tube. Then the annealing temperature was increased to 800 °C at a rate of 5 °C/min and maintained for 1 h in argon atmosphere. When the temperature was cooled down to room temperature, the final product was taken out of the corundum tube. When changing the mass ratio of graphite oxide: melamine, NG products with different nitrogen content can be obtained.

2.4. Preparation of NG modified GCE

GCE was polished successively using 0.3 μm and 0.05 μm Al_2O_3 powder and rinsed thoroughly with ethanol and water each for 5 min, and then dried with blowing N_2. 5 mg NG was dispersed in DMF by ultrasonication, and resulted in 1 mg/mL suspension. A 5 μL NG suspension was then pippetted onto the pretreated GCE surface and dried at room temperature.

3. Results and discussion

3.1. Characterization of the nitrogen doped graphene

Firstly, the surface morphology of the NG film modified on GCE was characterized by FE-SEM. As shown in Fig. 1a, the NG nanosheets are randomly packed on the GCE surface with folded or stacked structures. Zoomed-in SEM image (inset of Fig. 1a) shows that the graphene sheets with lots of ripples are still observable, demonstrating the graphene structure remaining on the electrode surface. Similarly, the AFM image (Fig. 1b) shows that the exfoliated NG is of nanosheet-like structure with an average thickness of ~0.8 nm. In the low magnification TEM image of NG (Fig. S1a) the corrugated nanoflakes with thousands of square nanometers look like a veil of silk covered on the Cu grid.

Fig. S1b shows the Raman scattering spectrum of NG prepared with a graphite oxide:melamine mass ratio 1:10 at 800 °C. The high intensity of D band at ~1352 cm^{-1} indicates the existence of many defects in the NG layers. These defects can be ascribed to the destruction of sp^2 C and nitrogen doping (Yang et al., 2005). A sharp G band located at 1576 cm^{-1} is assigned to the E_{2g} phonon of sp^2 C atoms, which demonstrates that after nitrogen doping graphene basically maintains its unique two dimensional structure. The 2D band is the most characteristic feature in Raman spectrum of graphene (Ferrari et al., 2006). The broad 2D band corresponding to a few layers graphene structure appears at 2697 cm^{-1}, which further confirms the existence of graphene structures in the final products. X-ray photoelectron spectroscopy (XPS) was carried out to analyze the composition and chemical configuration of nitrogen atoms in NG. As shown in the survey scan spectrum of Fig. 1c, besides the core levels of C1 s and O1 s locating at ~284.7 eV and ~532.1 eV, N1 s signal is also observed at ~398.2 eV clearly. In the high resolution C1 s spectrum (Fig. S1c), the peak can be resolved into three components respectively located at ~284.7 eV (—C═C), 285.8 eV (—C═N), and 287.0 eV (—C—N). Similarly, after fitting based on shirley algorithm, N1 s peak can be fitted into three components (Fig. 1d). The intense peaks locate at 398.2 eV and 399.5 eV is assigned to nitrogen atoms with "pyridinic" and "pyrrolic" chemical structures, and the peak at 401.0 eV corresponds to N atoms linked with three carbon atoms at the same (denoted as "graphitic"

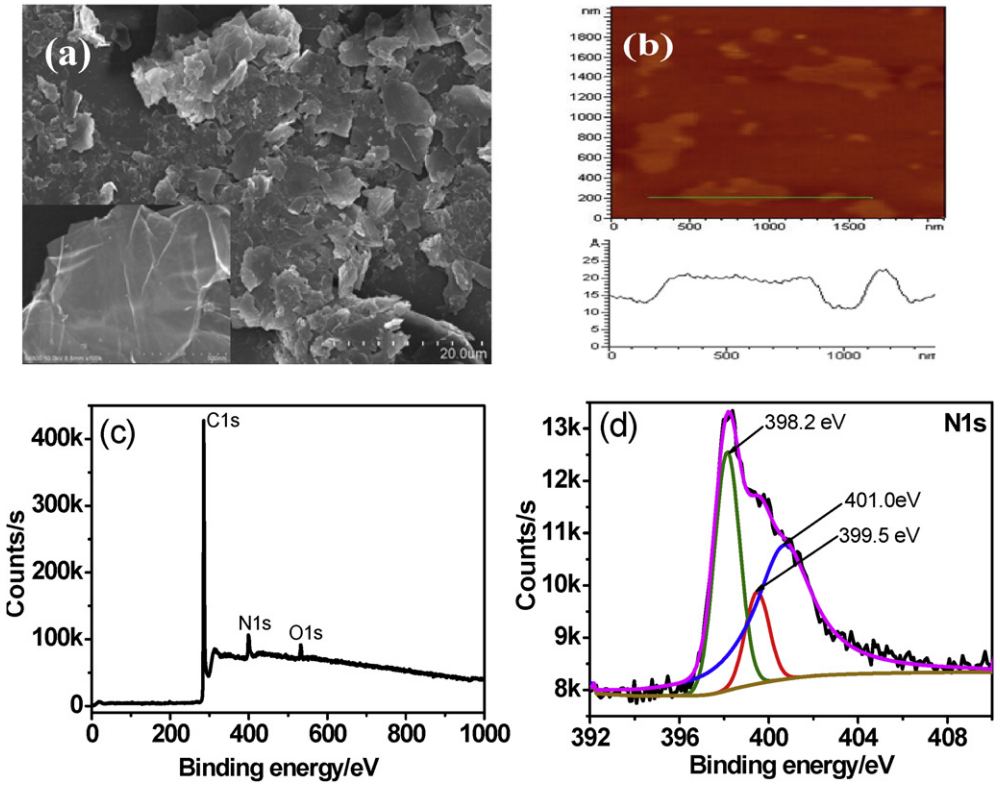

Fig. 1. (a) SEM image of the nitrogen doped graphene modified GCE with enlarged image as inset. (b) AFM images of the exfoliated nitrogen doped graphene. XPS spectrum of the nitrogen doped graphene: survey scan (c) and high resolution scans for N1 s (d).

N atoms) (Matter et al., 2006; Maldonado and Stevenson, 2005). These XPS analyses reveal that nitrogen atoms have been successfully incorporated into graphene frameworks and exist as three kinds of chemical status in graphene layers. When changing the mass ratio of graphite oxide:melamine from 1:1 to 1:50, NGs with different nitrogen content can be obtained (Table S1).

3.2. Electrochemical behaviors of AA, DA and UA

The individual electrochemical behaviors of AA, DA and UA at a bare GCE and a NG/GCE were first investigated by cyclic voltammetry (CV) (Fig. 2a and Fig. S2a). In the case of AA, the oxidation peak corresponds to the oxidation of hydroxy groups to carbonyl groups in furan ring of AA on NG/GCE. Because AA at pH 6.0 is negatively charged ($pK_{a,AA} = 4.1$), the enhanced electron transfer kinetics at the NG/GCE may be due to the formation of hydrogen bonds between the ascorbate and graphene layers in NG films. For DA, the appearance of a well defined redox couple with a 55 mV peak separation shows the reversibility of DA on the NG/GCE is much better than on bare GCE ($\Delta E = 215$ mV). This couple of redox peaks corresponds to two-electron oxidation of DA to dopaminequinone and the subsequent reduction of dopaminequinone to DA (Kalimuthu and John, 2009). The improved reversibility could be due to the π–π interactions between the benzene ring of DA molecule and graphene layer, and the hydrogen bonds formed between hydroxyl or amine group in DA molecule and nitrogen atoms within graphene layers. For UA, there appears a well-defined oxidation peak and a broad reduction peak on the NG/GCE. This CV curve reveals that UA is first oxidized to quinonoid, and then undergoes a rapid chemical reaction, which is considered as an EC mechanism (Safavi et al., 2006). In addition, it is found from the CV curves that the oxidation potentials are negatively shifted by 500 mV, 140 mV and 84 mV, respectively and the peak currents increase by about three times as compared to bare GCE. So graphene doped with nitrogen atoms can accelerate the electron transfer and decrease the overpotential of UA oxidation as well. It is obvious that AA, DA and UA molecules with different structure have different interaction modes with NG. As a result, NG can decrease the overpotentials of AA, DA and UA oxidation at different levels according to their interaction modes, which is the key factor to realize simultaneous determination AA, DA and UA.

The excellent electrocatalytic activity of NG towards the oxidation of these three biomolecules is also investigated by the differential pulse voltammetry (DPV) experiments (Fig. 2b) with a mixture of 1.0 mM (AA), 0.05 mM (DA) and 0.1 mM (UA) in 0.1 M PBS (pH 6.0). At the bare GCE, the electrooxidation of the three biomolecules presents only a small broad peak so that simultaneous determination of these molecules is impossible. On the contrary, on the NG/GCE three well defined oxidation peaks with larger peak separations and peak currents corresponding to the oxidation of AA, DA and UA appear, respectively, confirming that NG with much higher electrocatalytic activity can be used to construct electrochemical sensor for simultaneous determination AA, DA and UA. Both the CV and DPV experiments demonstrate that NG possesses good electrocatalytic activity towards the oxidation of these molecules. The highly electrocatalytic activity of NG could be due to the fact that nitrogen atoms in NG layers may interact with these molecules via hydrogen bond, which can activate the hydroxy and amine groups and accelerate the charge transfer kinetics of these molecules at NG surface. At the same time, the π–π interactions between graphene layers and these molecules can also promote the charge transfer of the three molecules (Wang et al., 2009b). Consequently, the observed fast heterogeneous electron kinetics of these three molecules on NG can be attributed to its particular two dimensional microstructure and properties originating from nitrogen doping.

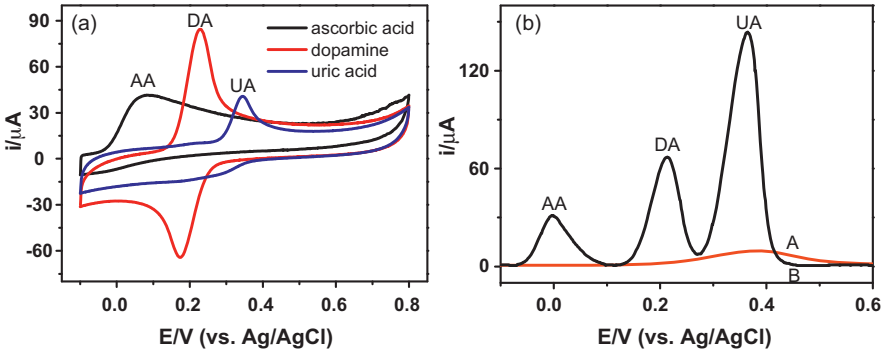

Fig. 2. (a) Cyclic voltammograms (CVs) of 1.0 mM AA, 1.0 mM DA and 1.0 mM UA in 0.10 M PBS (pH 6.0) at NG modified GCE at a scan rate of 100 mV/s. (b) Differential pulse voltammograms (DPVs) for 1.0 mM AA, 0.05 mM DA and 0.10 mM UA in a 0.1 M PBS (pH 6.0) at bare GCE (A) and NG/GCE (B), respectively.

As we know the nitrogen doping level could manipulate the electronic properties of NG and then alter the electrocatalytic activity of graphene. This is exactly observed from the DPVs of AA, DA and UA on NGs with different nitrogen doping level. Fig. S3 shows that the catalytic oxidation currents for AA (0.5 mM), DA (0.1 mM) and UA (0.1 mM) increase significantly with the increase of nitrogen doping level from 5.6% to 8.4% of NG products. However, peak potentials for the oxidation AA, DA and UA keep nearly unchanged. The potential differences among these biomolecules are in the range of 194–200 mV ($\Delta E_{DA\text{-}AA}$), 124–132 mV ($\Delta E_{UA\text{-}DA}$). So we suggest that it is not the peak potentials but peak currents for the oxidation AA, DA and UA that are influenced by the nitrogen doping level in graphene. In addition, it may imply that the pyridine-like nitrogen component determines the electrocatalytic activity of NGs towards the oxidation of AA, DA and UA because nitrogen bonding configurations in all NG samples in the present work are composed mainly of pyridinic nitrogen, which is similar to the results in ORR application (Sheng et al., 2011). According to the above results, NG with 8.4% (at.%) nitrogen content was used to simultaneously determine AA, DA and UA using DPV approach in the following experiments.

3.3. Effects of scan rate and pH on the electrochemistry of AA, DA and UA

The effect of scan rate on the CV responses of AA, DA and UA at the NG/GCE was studied. As shown in Fig. S4 the oxidation peak currents of AA, DA and UA increase with increasing the scan rate, while their oxidation peak potentials gradually shift to positive values. Plots of the anodic peak currents as a function of the square root of scan rate in the range of 5–500 mV/s show linear relationships, which indicates the electrode reactions of these three molecules are diffusion-controlled processes.

The influence of solution pH on the peak currents and peak potentials of the electrocatalytic oxidation of AA (500 μM), DA (100 μM) and UA (100 μM) at the NG/GCE was also investigated by DPV in the pH range of 3–7.4 (Fig. S5a). It is clear that with the increase of solution pH the oxidation peak potentials of the three molecules shift to negative values. Linear relationships of the peak potential of DA, UA and AA as function of solution pH with slopes of 62.2, 64.7 and 47.0 mV/pH, respectively are observed (Fig. S5b), indicating protons are directly involved in the overall oxidation reactions, i.e., the oxidation reactions occur via electron-transfer step followed by protonation process. The electrochemical oxidation of DA and UA has been proven to be a two-electron process, thus, the numbers of protons involved in their oxidation should also be two. While for AA, a slope of 47.0 mV/pH is relatively lower than that expected from the Nernst equation, which may suggest that the electrochemical oxidation of AA on the NG/GCE occur with less than one proton involved. Moreover, it is found that the oxidation peak currents increase with the solution pH in the range of 3–6 and then decrease when solution pH increases further to 7.4. The decrease at high solution pH could be due to the electrostatic repulsion between AA (UA) and NG nanosheets since AA ($pK_a = 4.1$) and UA ($pK_a = 5.7$) will be deprotonated at solution pH > 6 (Kalimuthu and John, 2010). On the contrast, the oxidation peak current of DA ($pK_a = 8.8$) gradually increases with the solution pH in the whole studied solution pH (3–7.4) since no deprotonation process occurs in the studied solution pH range. Furthermore, it is clear that the oxidation peak separations among the three molecules are larger than 170 (AA/DA), 120 (DA/UA), and 291 mV (AA/UA) in the studied pH range of 3.0–7.4. Therefore, individual and/or simultaneous detections of AA, DA and UA from their mixed solutions can be realized at the NG/GCE in a wide solution pH range. If considering the separation effect and detection sensitivity, the buffer solution pH of 6.0 was chosen in the following measurements.

3.4. Simultaneous/individual determination of AA, DA and UA on NG/GCE

For individual determination of AA, DA and UA at the NG/GCE, DPV was carried out in the potential range of −0.1 to 0.6 V in PBS (pH 6.0). In these measurements, only concentration of the target biomolecule was changed, while concentrations of the other two biomolecules were kept constant. As shown in Fig. 3, the electrochemical response of AA, DA, or UA increases linearly with the increase of the target biomolecule concentration. The linear ranges for the determination of AA, DA and UA are 5.0×10^{-6} to 1.3×10^{-3} M, 5.0×10^{-7} to 1.7×10^{-4} M and 1.0×10^{-7} to 2.0×10^{-5} M with detection limit of 2.2×10^{-6} M, 2.5×10^{-7} M and 4.5×10^{-8} M at $S/N = 3$, respectively. It is also found that addition of the target biomolecules into the electrochemical cell does not have significant influence on the peak currents and peak potentials of the other two biomolecules. The present results are compared to those in literature (Table 1). It clearly shows that the analytical parameters including detection limit and linear range using NG/GCE are better or comparable to the results reported for simultaneous determination of these biomolecules at different modified electrode surfaces.

The excellent electrocatalytic activity of NG also promises to simultaneous determination of AA, DA and UA using the NG/GCE. The electrochemical response of AA, DA or UA still increases linearly with the increase of their concentrations (Fig. 4). The corresponding linear ranges for AA, DA and UA determination are 1.0×10^{-5} to 6×10^{-4} M, 1.0×10^{-6} to 1.4×10^{-4} M and 2.0×10^{-6}

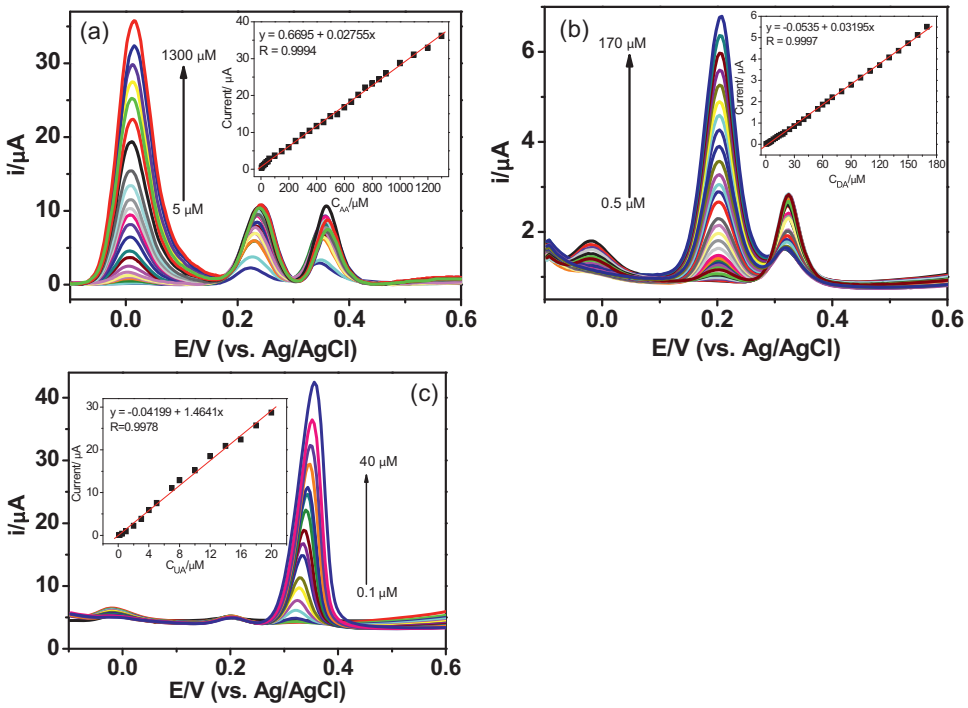

Fig. 3. DPV profiles at NG/GCE in 0.1 M PBS (pH 6.0) (a) containing 4 μM DA, 2 μM UA and different concentrations of AA from 5 μM to 1300 μM, (b) containing 100 μM AA, 5 μM UA and different concentrations of DA from 0.5 μM to 170 μM, and (c) containing 100 μM AA, 5 μM DA and different concentrations of UA from 0.1 μM to 40 μM. Inset: plots of the anodic peak current as a function of AA, DA and UA concentrations.

to 1.6×10^{-4} M with detection limit of 3.5×10^{-6} M, 2.8×10^{-7} M and 5.7×10^{-7} M at $S/N = 3$, respectively. These results demonstrate that individual or simultaneous determination of these biomolecules on NG/GCE can be achieved with high sensitivity and selectivity. The lower detection limit and wider linear range are due to the excellent electrocatalytic activity of NG itself towards these biomolecules. Thus, NG nanosheets with unique structural and electrocatalytic properties are promising candidate for construction of sensitive and selective biosensors, bioelectronics and biofuel cells.

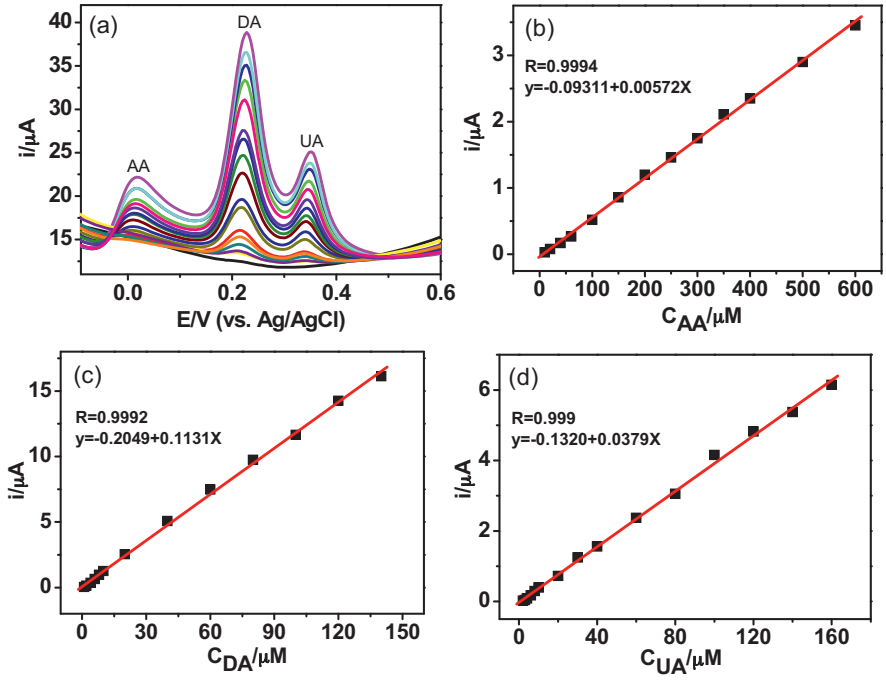

Fig. 4. (a) DPV profiles at NG/GCE in 0.1 M PBS (pH 6.0) containing different concentrations of AA, DA and UA. From bottom to up the concentrations from 10 to 1600 μM for AA, 1 to 200 μM for DA and 1 to 200 μM for UA, respectively. (b)–(d) Plots of the oxidation peak currents as a function of AA, DA and UA concentrations, respectively.

Table 1
The detection limits and linear ranges of different modified electrodes for the determination of AA, DA and UA.

Electrode materials	Detection limit (μmol L^{-1})			Linear range (μmol L^{-1})			Ref.
	AA	DA	UA	AA	DA	UA	
MWCNT/CCE[a]	7.71	0.31	0.42	15–800	0.5–100	0.55–90	Habibia and Pournaghi-Azar (2010)
CNF-CPE[b]	2	0.04	0.2	2–64	0.04–5.6	0.8–16.8	Liu et al. (2008b)
PGE[c]	13	0.11	1.4	25–500	1–20	2.5–30	da Silva et al. (2008)
OMC/Nafion[d]	20	0.5	4.0	40–800	1–90	5–80	Zheng et al. (2009)
Graphene	–	2.64	–	–	4–100	–	Kim et al. (2010)
3D graphene nanoflake	–	0.17	–	–	1–50	–	Shang et al. (2008)
Pd/CNF-CPE[e]	15	0.2	0.7	50–4000	0.5–160	2–200	Huang et al. (2008)
ZnO/RM[f]	1.4	0.7	4.5	15–240	6–960	50–800	Tang et al. (2008)
Pt-Au hybrid	103	24	21	103–165	24–384	21–336	Thiagarajan and Chen (2007)
(p-ATD)[g]	2.01	0.33	0.19	30–300	5–50	10–100	Kalimuthu and John (2010)
Chitosan-graphene	50	1	2	50–1200	1–24	2–45	Han et al. (2010)
NG	2.2	0.25	0.045	5–1300	0.5–170	0.1–20	This work

[a] Multiwalled carbon nanotube modified carbon–ceramic electrode.
[b] Carbon nanofiber modified carbon paste electrode.
[c] Pyrolytic graphite activated electrodes.
[d] Ordered mesoporous carbon/Nafion composite film.
[e] Palladium nanoparticle- loaded carbon nanofiber modified carbon paste electrode.
[f] Zinc oxide-electrogenerated redox mediator hybrid film.
[g] Electropolymerized film of 2-amino-1,3,4-thiadiazole.

4. Conclusions

The present work shows that nitrogen doped graphene with an average thickness of ~0.8 nm has been successfully synthesized by thermally annealing the mixture of graphite oxide and melamine. It is found that the resultant nitrogen doped graphene shows excellent electrocatalytic activity towards the oxidation of ascorbic acid, dopamine and uric acid. Detailed electrochemical characterizations unravel the fact that the observed electrocatalytic activity is relating to the structure of target biomolecules, the interactions of hydrogen bond and π–π stack between the target biomolecules and nitrogen doped graphene, and the unique structural and properties of nitrogen doped graphene. In addition, the electrooxidation of these three biomolecules on the nitrogen doped graphene modified electrode shows three well defined oxidation peaks with larger peak separation. Therefore, a sensitive electrochemical sensor has been elaborated to individually or simultaneously determine these biomolecules from their mixture solution. The present work demonstrates that nitrogen doped graphene nanosheets are promising candidate for construction of sensitive and selective biosensors, bioelectronics and other catalytic applications.

Acknowledgements

This work was supported by the Grants from the National 973 Basic Research Program (2012CB933804), the National Natural Science Foundation of China (21035002), the National Science Fund for Creative Research Groups (21121091) and the Natural Science Foundation of Jiangsu province (BK2010009).

Appendix A. Supplementary data

Supplementary data associated with this article can be found, in the online version, at doi:10.1016/j.bios.2012.01.030.

References

Allen, M.J., Tung, V.C., Kaner, R.B., 2010. Chem. Rev. 110, 132–145.
Arrigoni, O., De Tullio, M.C., 2002. Biochim. Biophys. Acta - Gen. Subj. 1569, 1–9.
Banks, C.E., Crossley, A., Salter, C., Wilkins, S.J., Compton, R.G., 2006. Angew. Chem. Int. Ed. 45, 2533–2537.
Chen, Y., Guo, L.R., Chen, W., Yang, X.J., Jin, B., Zheng, L.M., Xia, X.H., 2009. Bioelectrochemistry 75, 26–31.
da Silva, R.P., Lima, A.W.O., Serrano, S.H.P., 2008. Anal. Chim. Acta 612, 89–98.
Deng, C.Y., Chen, J.H., Wang, M.D., Xiao, C.H., Nie, Z., Yao, S.Z., 2009a. Biosens. Bioelectron. 24, 2091–2094.
Deng, S.Y., Jian, G.Q., Lei, J.P., Hu, Z., Ju, H.X., 2009b. Biosens. Bioelectron. 25, 373–377.
Dutt, V.E., Mottola, H.A., 1974. Anal. Chem. 46, 1777–1781.
Elias, D.C., Nair, R.R., Mohiuddin, T.M.G., Morozov, S.V., Blake, P., Halsall, M.P., Ferrari, A.C., Boukhvalov, D.W., Katsnelson, M.I., Geim, A.K., Novoselov, K.S., 2009. Science 323, 610–613.
Ferrari, A.C., Meyer, J.C., Scardaci, V., Casiraghi, C., Lazzeri, M., Mauri, F., Piscanec, S., Jiang, D., Novoselov, K.S., Roth, S., Geim, A.K., 2006. Phys. Rev. Lett. 97, 187401.
Gong, K.P., Du, F., Xia, Z.H., Durstock, M., Dai, L.M., 2009. Science 323, 760–764.
Guo, H.L., Wang, X.F., Qian, Q.Y., Wang, F.B., Xia, X.H., 2009. ACS Nano 3, 2653–2659.
Guo, B.D., Liu, Q., Chen, E.D., Zhu, H.W., Fang, L., Gong, J.R., 2010a. Nano Lett. 10, 4975–4980.
Guo, S.J., Wen, D., Zhai, Y.M., Dong, S.J., Wang, E.K., 2010b. ACS Nano 4, 3959–3968.
Habibia, B., Pournaghi-Azar, M.H., 2010. Electrochim. Acta 55, 5492–5498.
Han, D.X., Han, T.T., Shan, C.S., Ivaska, A., Niu, L., 2010. Electroanalysis 22, 2001–2008.
Heien, M.L.A.V., Khan, A.S., Ariansen, J.L., Cheer, J.F., Phillips, P.E.M., Wassum, K.M., Wightman, R.M., 2005. Proc. Natl. Acad. Sci. U.S.A. 102, 10023–10028.
Huang, J., Liu, Y., Hou, H., You, T., 2008. Biosens. Bioelectron. 24, 632–637.
Jones, C.P., Jurkschat, K., Crossley, A., Compton, R.G., Riehl, B.L., Banks, C.E., 2007. Langmuir 23, 9501–9504.
Kalimuthu, P., John, S.A., 2009. Electrochim. Acta 55, 183–189.
Kalimuthu, P., John, S.A., 2010. Talanta 80, 1686–1691.
Kim, K.S., Zhao, Y., Jang, H., Lee, S.Y., Kim, J.M., Kim, K.S., Ahn, J.H., Kim, P., Choi, J.Y., Hong, B.H., 2009. Nature 457, 706–710.
Kim, Y.R., Bong, S., Kang, Y.J., Yang, Y., Mahajan, R.K., Kim, J.S., Kim, H., 2010. Biosens. Bioelectron. 25, 2366–2369.
Lee, S.U., Belosludov, R.V., Mizuseki, H., Kawazoe, Y., 2009. Small 5, 1769–1775.
Liu, A.L., Zhang, S.B., Chen, W., Lin, X.H., Xia, X.H., 2008a. Biosens. Bioelectron 23, 1488–1495.
Liu, Y., Huang, J., Hou, H., You, T., 2008b. Electrochem. Commun. 10, 1431–1434.
Maldonado, S., Stevenson, K.J., 2005. J. Phys. Chem. B 109, 4707–4716.
Matter, P.H., Zhang, L., Ozkan, U.S., 2006. J. Catal. 239, 83–96.
Panchakarla, L.S., Subrahmanyam, K.S., Saha, S.K., Govindaraj, A., Krishnamurthy, H.R., Waghmare, U.V., Rao, C.N.R., 2009. Adv. Mater. 21, 4726–4730.
Pang, S.P., Tsao, H.N., Feng, X.L., Müllen, K., 2009. Adv. Mater. 21, 3488–3491.
Pumera, M., 2007. Langmuir 23, 6453–6458.
Qu, L.T., Liu, Y., Baek, J.B., Dai, L.M., 2010. ACS Nano 4, 1321–1326.
Rao, C.N.R., Sood, A.K., Subrahmanyam, K.S., Govindaraj, A., 2009. Angew. Chem. Int. Ed. 48, 7752–7777.
Reina, A., Jia, X.T., Ho, J., Nezich, D., Son, H.B., Bulovic, V., Dresselhaus, M.S., Kong, J., 2009. Nano Lett. 9, 30–35.
Safavi, A., Maleki, N., Moradlou, O., Tajabadi, F., 2006. Anal. Biochem. 359, 224–229.
Shang, N.G., Papakonstantinou, P., McMullan, M., Chu, M., Stamboulis, A., Potenza, A., Dhesi, S.S., Marchetto, H., 2008. Adv. Funct. Mater. 18, 3506–3514.
Shao, Y.Y., Wang, J., Wu, H., Liu, J., Aksay, I.A., Lin, Y.H., 2010. Electroanalysis 22, 1027–1036.
Sheng, Z.H., Shao, L., Chen, J.J., Bao, W.J., Wang, F.B., Xia, X.H., 2011. ACS Nano 5, 4350–4358.
Tang, C.F., Kumar, S.A., Chen, S.M., 2008. Anal. Biochem. 380, 174–183.
Tang, L.H., Wang, Y., Li, Y.M., Feng, H.B., Lu, J., Li, J.H., 2009. Adv. Funct. Mater. 19, 2782–2789.
Thiagarajan, S., Chen, S.M., 2007. Talanta 74, 212–222.
Wang, X.R., Li, X.L., Zhang, L., Yoon, Y.K., Weber, P.K., Wang, H.L., Guo, J., Dai, H.J., 2009a. Science 324, 768–771.

Wang, Y., Li, Y., Tang, L.H., Lu, J., Li, J.H., 2009b. Electrochem. Commun. 11, 889–892.
Wang, S., Ang, P.K., Wang, Z.Q., Tang, A.L.L., Thong, J.T.L., Loh, K.P., 2010a. Nano Lett. 10, 92–98.
Wang, Y., Shao, Y.Y., Matson, D.W., Li, J.H., Lin, Y.H., 2010b. ACS Nano 4, 1790–1798.
Xu, X., Jiang, S.J., Hu, Z., Liu, S.Q., 2010. ACS Nano 4, 4292–4298.
Yang, Q.H., Hou, P.X., Unno, M., Yamauchi, S., Saito, R., Kyotani, T., 2005. Nano Lett. 5, 2465–2469.
Zheng, D., Ye, J., Zhou, L., Zhang, Y., Yu, C., 2009. J. Electroanal. Chem. 625, 82–87.
Zhou, C.W., Kong, J., Yenilmez, E., Dai, H.J., 2000. Science 290, 1552–1555.
Zhou, Y.G., Chen, J.J., Wang, F.B., Sheng, Z.H., Xia, X.H., 2010. Chem. Commun. 46, 5951–5953.